Title: H_2O_2 sulfenylates CHE linking local infection to establishment of systemic acquired resistance

Authors: Lijun Cao[1,2], Heejin Yoo[1,2,†], Tianyuan Chen[1,2], Musoki Mwimba[1,2], Xing Zhang[1,2], and Xinnian Dong[1,2,*]

Affiliations:

[1] Department of Biology, Box 90338, Duke University, Durham, NC 27708, USA

[2] Howard Hughes Medical Institute, Duke University, Durham, NC 27708, USA

[*]Corresponding author: xdong@duke.edu

[†]Current address: School of Biological Science, University of Utah, Salt Lake City, UT 84112, USA

Abstract: In plants, a local infection can lead to systemic acquired resistance (SAR) through increased production of salicylic acid (SA). For 30 years, the identity of the mobile signal and its direct transduction mechanism for systemic SA synthesis in initiating SAR have been hotly debated. We found that, upon pathogen challenge, the cysteine residue of transcription factor CHE undergoes sulfenylation in systemic tissues, enhancing its binding to the promoter of SA-synthesis gene, *ICS1*, and increasing SA production. This occurs independently of previously reported pipecolic acid (Pip) signal. Instead, H_2O_2 produced by NADPH oxidase, RBOHD, is the mobile signal that sulfenylates CHE in a concentration-dependent manner. This modification serves as a molecular switch that activates CHE-mediated SA-increase and subsequent Pip-accumulation in systemic tissues to synergistically induce SAR.

One Sentence Summary: RBOHD-generated H_2O_2 sulfenylates transcription factor CHE to establish systemic acquired resistance in plants.

Main Text:

Systemic acquired resistance (SAR) is an inducible immune mechanism in plants (*1-3*). Unlike the animal adaptive immunity, SAR is triggered by local immune responses against specific pathogen effectors, known as effector-triggered immunity (ETI), and confers long-lasting protection to the rest of plants against a wide range of pathogens. This fascinating signaling phenomenon and its potential application in agriculture for engineering broad-spectrum disease resistance in crops have led to intense investigation and the identification of salicylic acid (SA) as the required signal for SAR (*4-7*). Though exogenous application of SA and its synthetic analogs has been shown to induce SAR without the ETI (*8-10*), for biological induction of SAR, how the local ETI induces systemic synthesis of SA has remained a mystery for more than 30 years. Multiple compounds, such as methyl salicylate (MeSA) (*11*), azelaic acid (AzA) (*12*), dehydroabietinal (DA) (*13*), glycerol-3-phosphate (G3P) (*14*) and pipecolic acid (Pip)/N-hydroxypipecolic acid (NHP) (*15-17*), have been identified as potential SAR signals that are involved in the production of SA and defense-related responses. However, a direct link between these mobile signals and systemic SA synthesis is missing.

RESULTS

CHE is a transcription factor required for SA synthesis and resistance only in systemic tissues

To identify the missing link between local ETI and systemic production of SA, we focused on the plant circadian clock transcription factor (TF), CCA1 HIKING EXPEDITION (CHE), which was found in our previous study to be required not only for the diurnal basal SA synthesis, but also for pathogen-induced SA production in systemic tissues (*18*). To better understand the regulation of CHE and how it contributes to the establishment of SAR over time, we performed time-course RNA-mediated oligonucleotide Annealing, Selection, and Ligation with next-generation sequencing (RASL-seq) (*19*) in both infected local and naïve systemic tissues. To minimize background variations between leaves, we used infected half-leaf as local tissues (Local) and the uninfected half-leaf as systemic tissues (Systemic), similar to the classic SAR experiment conducted by A. Frank Ross (*3*). After challenging *Arabidopsis thaliana* plants with the bacterial pathogen *Pseudomonas syringae* pv. *maculicola* (*Psm*) ES4326 carrying the effector gene *avrRpt2* (*Psm* ES4326/avrRpt2), the expression patterns of approximately 700 selected genes, with a particular focus on those involved in defense and SA production, were examined. We found similar overall gene expression patterns, as well as comparable levels of SA and Pip, in the *che* mutant compared to the wild type (WT) plants in the local tissues (Fig. 1, A and B, and fig. S1A). This finding is consistent with the previously reported normal local defense phenotype of the *che* mutant (*18*). However, in systemic tissues, the expression patterns were significantly different between WT and *che*, with the mutant showing lower gene inductions and substantial decreases in the production of SA and Pip (Fig. 1, A and B). These results show that TF CHE is required for SAR-associated gene expression and accumulation of SA and Pip only in systemic tissues. Interestingly, based on the RASL-seq data, the CHE-mediated systemic responses were not linked with significant transcriptional difference between WT and the *che* mutant of known TF genes *CALMODULIN BINDING PROTEIN 60G* (*CBP60g*) and *SAR DEFICIENT 1* (*SARD1*), which are involved in SA synthesis (*20*), *CIRCADIAN CLOCK-ASSOCIATED 1* (*CCA1*), which is a target clock gene of CHE (*21*), or *RESPIRATORY BURST OXIDASE HOMOLOGUE D* (*RBOHD*), which is known for immune-induced apoplastic ROS production (*22-26*) (fig. S1B).

We next examined effects of the *che* mutant on the transportation and sensing of SAR-inducing signal(s) by measuring the SAR-inducing activity of petiole exudates (PeX) as previously described (*27-29*). Notably, PeX derived from WT and *che* mutant after *Psm* ES4326/avrRpt2 treatment exhibited similar capacities in reducing bacterial growth in WT plants (Fig. 1C). This observation suggests that the *che* mutant can produce SAR-inducing mobile signals like the WT. However, the inability of *che* mutant to restore defense through the application of PeX from either WT or *che* after pathogen challenge (Fig. 1C) indicates that CHE is defective in sensing the mobile signal. Consequently, these findings further confirm that CHE is specifically required for SA synthesis and resistance in systemic tissues.

Cysteine mutants of CHE are defective in SAR

Since neither the *CHE* transcript nor the protein showed a significant increase in systemic tissues upon induction (fig. S2, A and B), we considered protein modification as an activation mechanism because CHE, also named TCP21, is one of the Class I TCP (TEOSINTE BRANCHED1, CYCLOIDEA, and PCF) TFs, which have a conserved cysteine residue in the non-canonical basic helix-loop-helix (bHLH) DNA-binding domain (*30*). Given that the cysteine-containing TCP proteins have been shown to be sensitive to redox conditions for their DNA-binding activity under different types of oxidants (*31*), and the cysteine residue of CHE is conserved across many plant species (fig. S2C), we decided to test whether mutating the single cysteine residue of CHE (cysteine 51) alters its function in SAR. We found that, unlike the WT *CHE* expressed by its native promoter (*CHEC*), the cysteine mutants che^{CS} (cysteine to serine) and che^{CW} (cysteine to tryptophan) failed in rescuing the SAR deficiency of the *che* mutants (Fig. 2, A and B, and fig. S3A) (*18*). This was accompanied by compromised systemic inductions of the SA synthesis gene *ISOCHORISMATE SYNTHASE 1* (*ICS1*), the SA-responsive gene *PATHOGENESIS-RELATED GENE 1* (*PR1*), and the Pip/NHP-synthesis genes *AGD2-LIKE DEFENSE RESPONSE PROTEIN 1* (*ALD1*) and *FLAVIN-DEPENDENT MONOOXYGENASE 1* (*FMO1*) (*32*) (fig. S3, B to E) and lower production of SA and Pip (Fig. 2, C and D) observed in the cysteine mutant line.

To examine the effect of the cysteine-mutant on the transcriptional activity regulated by CHE, we performed chromatin immunoprecipitation-quantitative PCR (ChIP-qPCR) analysis and found that after pathogen challenge, the binding of CHE to the *ICS1* promoter ($ICS1_p$), which carries the TCP-binding site, was significantly increased in the systemic tissues of *CHEC* transgenic plants, while this increase was compromised in the transgenic plants expressing che^{CS} (Fig. 2E). We also performed exogenous SA treatment and observed a similar defect in SA-induced promoter-binding for the che^{CS} mutant protein (Fig. 2F), consistent with our previous work showing that the *che* mutants are defective in SA-mediated signal amplification (*18*). However, the binding of CHE to the clock gene *CCA1* promoter (*CCA1p*), which also carries a TCP-binding site (*21*), was not significantly increased after pathogen challenge (Fig. 2G) nor after SA treatment (Fig. 2H). Consistent with our observations that the che^{CS} mutant could rescue the short period of *CCA1* expression (*21*) in the *che-1 lhy-20* double mutant (fig. S4, A and B). These data indicate that CHE regulates systemic SA synthesis independent of its clock function. Furthermore, we found that CHE does not bind to the promoter of *ALD1* or *FMO1* (fig. S5, A and B), suggesting that the regulation of SAR by CHE is not directly through these genes. Taken together, these results demonstrate that the cysteine residue of CHE regulates SA synthesis in systemic tissues through the modulation of its binding to the *ICS1* promoter.

112 **CHE-mediated SA synthesis in systemic tissues occurs prior to and independent of the Pip**
113 **increase**

114 SA and Pip are both important molecules that regulate SAR upon pathogen infection (*4, 16, 32*)
115 and the systemic induction of both molecules are compromised in *che* mutants (Fig. 1B, and Fig.
116 2, C and D). Pip is one of the early accumulated signals and it was shown to function upstream of
117 many other SAR-inducing signals, including AzA and G3P, upon pathogen challenge (*33-35*).
118 Therefore, it is important to know whether Pip is induced earlier than SA during the initiation of
119 SAR. We performed a time-course measurement of SA and Pip levels in both local and systemic
120 tissues. The results showed that SA and Pip were significantly increased in the local tissues 12
121 hours post pathogen infiltration (Fig. 2, I and J). However, in the systemic tissues, at 12 hours post
122 pathogen infiltration, SA level was elevated (Fig. 2K), whereas Pip was not (Fig. 2L), suggesting
123 that the initial systemic induction of SA might not be through the Pip pathway, consistent with a
124 previous report that *de novo* synthesis of Pip in systemic tissues is dependent on SA (*33*).
125 Moreover, induction of the SA synthesis gene *ICS1* was observed in systemic tissues at 8 hours
126 post pathogen infiltration, whereas an increase in the Pip synthesis gene *ALD1* was not detected
127 even at 12 hours post pathogen infiltration (Fig. 2, M and N). These results indicate that systemic
128 inductions of *ICS1* and SA production by CHE occur prior to Pip induction. In our analysis, the
129 Pip derivative NHP was not detected despite that we successfully detected NHP standard, probably
130 due to instability of NHP as suggested by previous studies (*15, 36*).

131 **CHE is sulfenylated in systemic tissues after a local induction of ETI**

132 To investigate how CHE initiates SAR, we focused on its functionally important cysteine residue.
133 The thiol moiety (-SH) of cysteine residue is highly reactive and can undergo various
134 modifications by reactive oxygen species (ROS), including forming disulfide bond between two
135 cysteines, S-sulfenylation (SOH), S-sulfinylation (SO_2H) and S-sulfonylation (SO_3H) (*37*). Since
136 CHE has only one cysteine residue, a disulfide bond formation would require a cysteine-containing
137 partner which was not detected under either mock or induced conditions using non-reducing SDS
138 gel electrophoresis (fig. S2B). We then performed a biotin-switch assay (*38*) to examine other
139 possible modifications. Excitingly, we found that CHE is specifically sulfenylated (CHE-SOH) in
140 the systemic tissues between 8 and 36 hours post infiltration with *Psm* ES4326/avrRpt2, but not
141 from mock-treatment (Fig. 3A, and fig. S6A). In addition, we found CHE in the distal systemic
142 tissues also underwent sulfenylation when lower leaves were challenged with *Psm*
143 ES4326/avrRpt2 (fig. S6B). This confirms that both the adjacent and distal systemic tissues
144 employ similar mechanism in establishing SAR as suggested in the classic study (*3*). In addition,
145 exogenous application of SA could also lead to CHE-SOH, though later at 24 hours after the
146 treatment (Fig. 3A). To determine whether CHE can be sulfenylated *in vitro*, we treated purified
147 CHE with various concentrations of H_2O_2, as H_2O_2 is known to be produced during plant defense
148 responses including ETI (*39, 40*). Interestingly, we found that CHE is sulfenylated specifically at
149 50 μM H_2O_2 treatment, while lower or higher concentrations did not result in sulfenylation (Fig.
150 3B).

151 To determine whether the *in vivo* CHE-binding to the *ICS1* promotor (Fig. 2E) is due to
152 sulfenylation of its cysteine residue, we performed a gel electrophoresis mobility shift assay using
153 a DNA probe containing the TCP-binding site from the *ICS1* promoter (*TBSi*). We found that
154 treatment with 50 μM H_2O_2 significantly enhanced the binding of CHE to *TBSi in vitro* (Fig. 3C).
155 This increase in promoter-binding is specific to CHE-SOH because treatment of H_2O_2-induced

156 CHE with the specific reducing agent for the sulfenic acid, sodium arsenite (m-arsenite),
157 diminished the binding, similar to the general reducing agent DTT treatment (Fig. 3, B and C).
158 Moreover, the H_2O_2-induced binding was largely absent in the che^{CS} mutant protein (Fig. 3C),
159 which further confirmed that sulfenylation of the cysteine residue in CHE is the molecular switch
160 that increases its binding to the *ICS1* promoter.

161 To address the question why CHE sulfenylation is only detected in systemic tissues, we
162 hypothesized that, as suggested by our H_2O_2-concentration-dependent sulfenylation experiment
163 (Fig. 3B), the higher ROS levels in the local tissues might cause further oxidation of the cysteine
164 residue in CHE. We found that this was indeed the case because sulfinylation (CHE-SO_2H) was
165 detected in the local tissues while sulfenylation (CHE-SOH) in systemic tissues (Fig. 3, D and E).
166 Regardless of whether CHE-SO_2H in the local tissues can be further oxidized to CHE-SO_3H,
167 neither form is active in binding to the *ICS1* promoter as shown by the ChIP-qPCR results (Fig.
168 3F). This H_2O_2-concentration-specific activation of CHE also explains the different conclusions
169 on the role of H_2O_2 observed in previous studies which utilized different H_2O_2 concentrations (*41,*
170 *42*).

171 **Production of H_2O_2 by RBOHD during ETI serves as a mobile signal for SAR**

172 Since *in vitro* treatment of CHE protein by H_2O_2 can cause its sulfenylation, we investigated the
173 possibility of H_2O_2 serving as the endogenous signal for activating CHE by measuring H_2O_2 levels
174 in both local and systemic tissues after a local ETI induction. As expected, we detected higher
175 induction of H_2O_2 levels in the local tissues than in the systemic tissues from 4 hours post pathogen
176 infiltration (Fig. 4A, and fig S7, A and B). The increased production of H_2O_2 in distal systemic
177 tissues starts around 8 hours post pathogen challenge in the lower leaves (fig. S7C). Interestingly,
178 this H_2O_2 increase was not significantly affected in the *che* mutant, except at 24 hours post
179 pathogen infiltration in the systemic tissues (Fig. 4A, and fig S7, A and B), nor in the *ald1* or *fmo1*
180 mutants; but abolished in *rps2,* the receptor *RESISTANT TO P. SYRINGAE 2* mutant for the
181 bacterial effector avrRpt2 (*43, 44*); in *sid2,* a *SALICYLIC ACID INDUCTION DEFICIENT 2*
182 mutant in the SA-synthesis gene *ICS1 (45)*; and in *rbohD*. Consistently, H_2O_2 levels in petiole
183 exudates collected from the *che*, *ald1* and *fmo1* mutant plants were similarly increased as in the
184 WT, while those from the *rbohD* and *rps2* mutants showed no increase (Fig. 4B). These results
185 demonstrate that the production of H_2O_2 during defense does not require the previously reported
186 mobile signals Pip or NHP (*15, 17, 33*) but requires RBOHD and the receptor for the effector
187 RPS2. Moreover, SA treatment could also induce production of H_2O_2 to a level similar to that
188 detected in systemic tissues induced by ETI (fig. S7D). This indicates the involvement of SA in
189 the production of H_2O_2, which is consistent with the previous reports (*34, 41*) and the observation
190 that ETI-induced H_2O_2 production is compromised in the SA-deficient *sid2* mutant (fig. S7, A and
191 B).

192 The requirement of the RPS2 immune receptor for the production of H_2O_2 during SAR is
193 noteworthy because while induction of SAR was initially reported to be associated with necrosis
194 in the local tissues (*3, 46*), there have been reports showing induction of systemic resistance by
195 virulent pathogens that do not trigger visually detectable cell death (*16, 47-49*). Therefore, we used
196 the type III secretion system mutant *Ps pv. tomato* (*Pst*) DC3000 *hrcC*$^-$, which is unable to deliver
197 effectors to the plant host (*50*), to examine the sulfenylation of CHE in systemic tissues. Our results
198 revealed that, under the same inoculation conditions, *Pst* DC3000 *hrcC*$^-$ failed to induce systemic
199 CHE-SOH or the expression of *ICS1* or *PR1,* unlike the *Pst* DC3000/avrRpt2 control (fig. S7, E

to G). These findings suggest that a strong and sustained production of H_2O_2 in local tissues is required for the establishment of SAR.

To monitor the transportation of ROS, including H_2O_2, from the local to systemic tissues during SAR induction, we employed a live imaging technique using 2',7'-dichlorodihydrofluorescein diacetate (*51, 52*). Upon pathogen challenge, strong ROS signals were detected in both WT and *ald1* plants in the local tissues, and the transportation of ROS signal(s) to systemic tissues was subsequently observed in both genetic backgrounds (Fig. 4C, and Movies S1 and S2), indicating that ROS (e.g., H_2O_2) signaling is not directly dependent of production of Pip/NHP. Moreover, the induced ROS production occurred earlier following pathogen challenge in both local and systemic tissues than other reported mobile signals, such as G3P, AzA, DA and Pip (*32, 35*) (Fig. 4C, and Movies S1 and S2). However, we observed a marked reduction in ROS production and transportation in the *rbohD* mutant (Fig. 4C, and Movie S3), consistent with the diminished H_2O_2 levels observed in this mutant in our quantitative measurements (Fig. 4B, and fig. S7, A and B). RBOHD is known to catalyze the production of H_2O_2 by transfer electrons to oxygen to form superoxide anion (O_2^-) which is subsequently converted to H_2O_2 through enzymatic or non-enzymatic dismutation (*53*). Furthermore, in the *rbohD* mutant, we observed a deficiency of CHE-SOH (Fig. 4D) and reduced CHE binding to the *ICS1* promoter (fig. S8A), as well as compromised induction of *ICS1* and systemic-induced resistance to *Psm* ES4326 (fig. S8, B and C). Based on these findings, we hypothesized that RBOHD-produced H_2O_2 during ETI is a mobile signal for the establishment of SAR.

H_2O_2 in petiole exudates is responsible for sulfenylation of CHE, SA synthesis, and induction of resistance in systemic tissues

We next examined whether H_2O_2 is the signal that sulfenylates CHE and establishes SAR in naïve tissues. We found that pretreating the petiole exudates collected from WT and the *fmo1* mutant with the H_2O_2-scavenging enzyme, catalase (CAT), led to depletion of H_2O_2 (fig. S8D). This treatment also inhibited the exudate's ability in sulfenylating CHE (Fig. 4E) and inducing the expression of *ICS1* (Fig. 4F), *ALD1*, *FMO1* and *PR1* (fig. S8, E to G), and in triggering resistance against *Psm* ES4326 (Fig. 4G). This inhibitory effect of catalase was abolished by heat denaturation (CAT_{boil}) and could be overcome by exogenous application of H_2O_2 after removing the enzyme (Fig. 4, E to G, and fig S8, E to G). These results further support our hypothesis that H_2O_2 production mediated by RBOHD is the initiating mobile signal that activates CHE through sulfenylation to induce SAR. It is interesting that, compared to the petiole exudates collected from WT, those collected from the *fmo1* mutant were less active in inducing *ALD1* and *FMO1* genes (fig. S8, E and F) and in conferring resistance to *Psm* ES4326 (Fig. 4G), consistent with the reduced sulfenylation of CHE in *sard1,* a mutant that affects SA and Pip synthesis (*20, 54*), in *ald1* and *fmo1* mutants (Fig. 4D). These results suggest the existence of mutual amplifications between SA and Pip/NHP signaling in systemic tissues which is consistent with the previous reports that Pip/NHP, together with SA, play an important role in the establishment of SAR (*32*). It is interesting that while PeX collected from WT after pathogen challenge-initiated defense against *Psm* ES4326 in both the treated and distal leaves of WT plants, it only triggered defense in the treated leaves of *rbohD* plants (Fig. 4H), indicating that distal SAR requires the transport or relay-production of H_2O_2 by this membrane-associated NADPH oxidase.

242 In summary, H_2O_2 produced through RBOHD during ETI is the primary signal that
243 sulfenyaltes CHE and induces the expression of *ICS1*, which directly results in *de novo* synthesis
244 of SA in systemic tissues. H_2O_2-mediated sulfenyaltion of CHE is required for SA and Pip
245 accumulation in the systemic tissues and both signals function synergistically to fully induce SAR
246 (Fig. 4I).

247 **Discussion**

248 It is intriguing that a circadian clock TF (i.e., CHE) is used to control SAR in plants. It raises
249 questions about the biological significance of this phenomenon. Since the redox-sensitive cysteine
250 residue in CHE is highly conserved among plant species (fig. S2C), it is likely that H_2O_2-mediated
251 sulfenylation and activation of CHE for SAR is a conserved mechanism in plants. Interestingly,
252 the mutation of the cysteine residue in CHE does not affect its clock function (Fig. 2, G and H,
253 and fig. S1B and S4), indicating that the crucial role of CHE in SAR is a novel function beyond
254 circadian clock regulation. Therefore, the significance of CHE's role in SAR probably lies upon
255 its own diurnal expression, which peaks around dusk (*18, 55*) (fig. S2A). Indeed, we have shown
256 in a separate study that ETI-associated cell death is gated by the redox rhythm towards the morning
257 (*56*). Therefore, the peak expression of CHE around dusk coincides with its sulfenylation at 8-12
258 hours after the morning induction of ETI (Fig. 3A) and also consistent with CHE-mediated basal
259 SA synthesis which occurs at night and reaches the maximum before dawn (*18*).

260 The discovery of H_2O_2 produced during ETI as the initiating mobile signal and H_2O_2-
261 mediated sulfenylation of CHE as the signal transduction mechanism explains "the classic" SAR
262 (*1-3, 57*) because of the requirement of RPS2-mediated ETI for the sulfenylation of CHE in
263 systemic tissues (Fig. 4D, fig. S7, E to G). However, studies have shown that infection by virulent
264 pathogens can also induce enhanced disease resistance in plant systemic tissues (*2, 48, 49*).
265 Whether these responses involve distinct induction mechanisms require further investigation. It is
266 conceivable that a long-lasting H_2O_2 production during a local induction event is the main
267 determining factor. Whereas microbe-associated molecular patterns (MAMPs)-treatment can
268 activate RBOHD and trigger apoplastic H_2O_2 production (*25, 53*), pathogen-induced ETI, which
269 involves the detection of both MAMP and effector signals, can lead to a strong and prolonged
270 H_2O_2 production (*58*). The more transient nature of the H_2O_2 increase during PTI might explain
271 the lack of systemic CHE sulfenylation and defense gene expression after a local inoculation by
272 *Pst* DC3000 *hrcC*$^-$, in contrast to the *Pst* DC3000/avrRpt2 (fig. S7, E to G). Therefore, the dose of
273 pathogen inoculant and the testing time after the initial induction may all have an impact on the
274 result. Our finding that an optimal concentration of H_2O_2 is required to sulfenylate CHE might
275 also reconcile conflicting reports on the role of H_2O_2 in defense (*41, 42*) because if a higher-than-
276 optimal level of H_2O_2 were used in treating plants, CHE would be inactivated through further
277 oxidation of the cysteine (Fig. 3, B to F, and 4A). It is tempting to hypothesize that the sensitivity
278 of CHE to H_2O_2 concentration would allow plants to gauge the level of local infection to determine
279 whether and how much to activate SAR in naïve tissues. Therefore, our study not only identifies
280 H_2O_2 as the initiating mobile signal and H_2O_2-concentration-dependent sulfenylation of CHE in
281 inducing *de novo* systemic SA synthesis as the signal transduction mechanism, but also conforms
282 with many discoveries made in the past 30 more years to show how a local infection modulates
283 the level of SAR (*1-3, 32*).

284

285 **References**

1. Z. Q. Fu, X. N. Dong, Systemic Acquired Resistance: Turning Local Infection into Global Defense. *Annu Rev Plant Biol* **64**, 839-863 (2013).
2. A. C. Vlot *et al.*, Systemic propagation of immunity in plants. *New Phytol* **229**, 1234-1250 (2021).
3. A. F. Ross, Systemic Acquired Resistance Induced by Localized Virus Infections in Plants. *Virology* **14**, 340-& (1961).
4. T. Gaffney *et al.*, Requirement of Salicylic-Acid for the Induction of Systemic Acquired-Resistance. *Science* **261**, 754-756 (1993).
5. B. Vernooij *et al.*, Salicylic-Acid Is Not the Translocated Signal Responsible for Inducing Systemic Acquired-Resistance but Is Required in Signal Transduction. *Plant Cell* **6**, 959-965 (1994).
6. J. Malamy, D. F. Klessig, Salicylic-Acid and Plant-Disease Resistance. *Plant J* **2**, 643-654 (1992).
7. J. P. Metraux *et al.*, Increase in Salicylic-Acid at the Onset of Systemic Acquired-Resistance in Cucumber. *Science* **250**, 1004-1006 (1990).
8. R. F. White, Acetylsalicylic-Acid (Aspirin) Induces Resistance to Tobacco Mosaic-Virus in Tobacco. *Virology* **99**, 410-412 (1979).
9. L. Friedrich *et al.*, A benzothiadiazole derivative induces systemic acquired resistance in tobacco. *Plant J* **10**, 61-70 (1996).
10. E. R. Ward *et al.*, Coordinate Gene Activity in Response to Agents That Induce Systemic Acquired-Resistance. *Plant Cell* **3**, 1085-1094 (1991).
11. S. W. Park, E. Kaimoyo, D. Kumar, S. Mosher, D. F. Klessig, Methyl salicylate is a critical mobile signal for plant systemic acquired resistance. *Science* **318**, 113-116 (2007).
12. H. W. Jung, T. J. Tschaplinski, L. Wang, J. Glazebrook, J. T. Greenberg, Priming in Systemic Plant Immunity. *Science* **324**, 89-91 (2009).
13. R. Chaturvedi *et al.*, An abietane diterpenoid is a potent activator of systemic acquired resistance. *Plant J* **71**, 161-172 (2012).
14. B. Chanda *et al.*, Glycerol-3-phosphate is a critical mobile inducer of systemic immunity in plants. *Nat Genet* **43**, 421-+ (2011).
15. Y. C. Chen *et al.*, N-hydroxy-pipecolic acid is a mobile metabolite that induces systemic disease resistance in Arabidopsis. *P Natl Acad Sci USA* **115**, E4920-E4929 (2018).
16. H. Navarova, F. Bernsdorff, A. C. Doring, J. Zeier, Pipecolic Acid, an Endogenous Mediator of Defense Amplification and Priming, Is a Critical Regulator of Inducible Plant Immunity. *Plant Cell* **24**, 5123-5141 (2012).
17. M. Hartmann *et al.*, Flavin Monooxygenase-Generated N-Hydroxypipecolic Acid Is a Critical Element of Plant Systemic Immunity. *Cell* **173**, 456-+ (2018).
18. X. Y. Zheng *et al.*, Spatial and temporal regulation of biosynthesis of the plant immune signal salicylic acid. *P Natl Acad Sci USA* **112**, 9166-9173 (2015).
19. H. Li, J. Qiu, X. D. Fu, RASL-seq for massively parallel and quantitative analysis of gene expression. *Curr Protoc Mol Biol* **Chapter 4**, Unit 4 13 11-19 (2012).
20. Y. X. Zhang *et al.*, Control of salicylic acid synthesis and systemic acquired resistance by two members of a plant-specific family of transcription factors. *P Natl Acad Sci USA* **107**, 18220-18225 (2010).
21. J. L. Pruneda-Paz, G. Breton, A. Para, S. A. Kay, A Functional Genomics Approach Reveals CHE as a Component of the Arabidopsis Circadian Clock. *Science* **323**, 1481-1485 (2009).

22. U. Dubiella *et al.*, Calcium-dependent protein kinase/NADPH oxidase activation circuit is required for rapid defense signal propagation. *P Natl Acad Sci USA* **110**, 8744-8749 (2013).
23. M. A. Torres, J. D. G. Jones, J. L. Dangl, Pathogen-induced, NADPH oxidase-derived reactive oxygen intermediates suppress spread of cell death in Arabidopsis thaliana. *Nat Genet* **37**, 1130-1134 (2005).
24. M. A. Torres, J. L. Dangl, Functions of the respiratory burst oxidase in biotic interactions, abiotic stress and development. *Current Opinion in Plant Biology* **8**, 397-403 (2005).
25. D. Lee *et al.*, Regulation of reactive oxygen species during plant immunity through phosphorylation and ubiquitination of RBOHD. *Nat Commun* **11**, (2020).
26. M. E. Alvarez *et al.*, Reactive oxygen intermediates mediate a systemic signal network in the establishment of plant immunity. *Cell* **92**, 773-784 (1998).
27. R. W. King, J. A. Zeevaart, Enhancement of Phloem Exudation from Cut Petioles by Chelating-Agents. *Plant Physiol* **53**, 96-103 (1974).
28. A. M. Maldonado, P. Doerner, R. A. Dixon, C. J. Lamb, R. K. Cameron, A putative lipid transfer protein involved in systemic resistance signalling in Arabidopsis. *Nature* **419**, 399-403 (2002).
29. P. Carella *et al.*, Comparative Proteomics Analysis of Phloem Exudates Collected during the Induction of Systemic Acquired Resistance. *Plant Physiol* **171**, 1495-1510 (2016).
30. S. Li, The Arabidopsis thaliana TCP transcription factors: A broadening horizon beyond development. *Plant Signal Behav* **10**, e1044192 (2015).
31. I. L. Viola, L. N. Guttlein, D. H. Gonzalez, Redox Modulation of Plant Developmental Regulators from the Class I TCP Transcription Factor Family. *Plant Physiol* **162**, 1434-1447 (2013).
32. M. Hartmann, J. Zeier, N-hydroxypipecolic acid and salicylic acid: a metabolic duo for systemic acquired resistance. *Curr Opin Plant Biol* **50**, 44-57 (2019).
33. C. X. Wang *et al.*, Pipecolic acid confers systemic immunity by regulating free radicals. *Sci Adv* **4**, (2018).
34. C. X. Wang *et al.*, Free Radicals Mediate Systemic Acquired Resistance. *Cell Rep* **7**, 348-355 (2014).
35. A. Kachroo, P. Kachroo, Mobile signals in systemic acquired resistance. *Current Opinion in Plant Biology* **58**, 41-47 (2020).
36. E. C. Holmes, Y. C. Chen, M. B. Mudgett, E. S. Sattely, Arabidopsis UGT76B1 glycosylates N-hydroxy-pipecolic acid and inactivates systemic acquired resistance in tomato. *Plant Cell* **33**, 750-765 (2021).
37. S. Ahmad *et al.*, Protein oxidation: an overview of metabolism of sulphur containing amino acid, cysteine. *Front Biosci (Schol Ed)* **9**, 71-87 (2017).
38. C. I. Murray, J. E. Van Eyk, Chasing Cysteine Oxidative Modifications Proteomic Tools for Characterizing Cysteine Redox Status. *Circ-Cardiovasc Gene* **5**, O1-O10 (2012).
39. E. Kuzniak, H. Urbanek, The involvement of hydrogen peroxide in plant responses to stresses. *Acta Physiol Plant* **22**, 195-203 (2000).
40. Y. Fichman, S. I. Zandalinas, S. Peck, S. Luan, R. Mittler, HPCA1 is required for systemic reactive oxygen species and calcium cell-to-cell signaling and plant acclimation to stress. *Plant Cell* **34**, 4453-4471 (2022).
41. Z. X. Chen, H. Silva, D. F. Klessig, Active Oxygen Species in the Induction of Plant Systemic Acquired-Resistance by Salicylic-Acid. *Science* **262**, 1883-1886 (1993).

42. U. Neuenschwander *et al.*, Is Hydrogen-Peroxide a 2nd-Messenger of Salicylic-Acid in Systemic Acquired-Resistance. *Plant J* **8**, 227-233 (1995).
43. A. F. Bent *et al.*, Rps2 of Arabidopsis-Thaliana - a Leucine-Rich Repeat Class of Plant-Disease Resistance Genes. *Science* **265**, 1856-1860 (1994).
44. M. Mindrinos, F. Katagiri, G. L. Yu, F. M. Ausubel, The a-Thaliana Disease Resistance Gene Rps2 Encodes a Protein Containing a Nucleotide-Binding Site and Leucine-Rich Repeats. *Cell* **78**, 1089-1099 (1994).
45. M. C. Wildermuth, J. Dewdney, G. Wu, F. M. Ausubel, Isochorismate synthase is required to synthesize salicylic acid for plant defence. *Nature* **414**, 562-565 (2001).
46. L. Sticher, B. MauchMani, J. P. Metraux, Systemic acquired resistance. *Annu Rev Phytopathol* **35**, 235-270 (1997).
47. R. K. Cameron, R. A. Dixon, C. J. Lamb, Biologically Induced Systemic Acquired-Resistance in Arabidopsis-Thaliana. *Plant J* **5**, 715-725 (1994).
48. T. E. Mishina, J. Zeier, Pathogen-associated molecular pattern recognition rather than development of tissue necrosis contributes to bacterial induction of systemic acquired resistance in Arabidopsis. *Plant J* **50**, 500-513 (2007).
49. P. P. Liu, S. Bhattacharjee, D. F. Klessig, P. Moffett, Systemic acquired resistance is induced by R gene-mediated responses independent of cell death. *Mol Plant Pathol* **11**, 155-160 (2010).
50. J. Yuan, S. Y. He, The Pseudomonas syringae hrp regulation and secretion system controls the production and secretion of multiple extracellular proteins. *J Bacteriol* **178**, 6399-6402 (1996).
51. Y. Fichman, G. Miller, R. Mittler, Whole-Plant Live Imaging of Reactive Oxygen Species. *Mol Plant* **12**, 1203-1210 (2019).
52. S. I. Zandalinas *et al.*, Systemic signaling during abiotic stress combination in plants. *P Natl Acad Sci USA* **117**, 13810-13820 (2020).
53. J. S. Qi, J. L. Wang, Z. Z. Gong, J. M. Zhou, Apoplastic ROS signaling in plant immunity. *Current Opinion in Plant Biology* **38**, 92-100 (2017).
54. T. J. Sun *et al.*, ChIP-seq reveals broad roles of SARD1 and CBP60g in regulating plant immunity. *Nat Commun* **6**, (2015).
55. T. C. Mockler *et al.*, The Diurnal Project: Diurnal and Circadian Expression Profiling, Model-based Pattern Matching, and Promoter Analysis. *Cold Sh Q B* **72**, 353-363 (2007).
56. S. Karapetyan, M. Mwimba, X. Dong, Circadian redox rhythm gates immune-induced cell death distinctly from the genetic clock. *bioRxiv*, (2023).
57. M. Grant, C. Lamb, Systemic immunity. *Current Opinion in Plant Biology* **9**, 414-420 (2006).
58. M. H. Yuan *et al.*, Pattern-recognition receptors are required for NLR-mediated plant immunity. *Nature* **592**, 105-+ (2021).
59. H. Navarova, F. Bernsdorff, A. C. Doring, J. Zeier, Pipecolic acid, an endogenous mediator of defense amplification and priming, is a critical regulator of inducible plant immunity. *Plant Cell* **24**, 5123-5141 (2012).
60. T. E. Mishina, J. Zeier, The Arabidopsis flavin-dependent monooxygenase FMO1 is an essential component of biologically induced systemic acquired resistance. *Plant Physiol* **141**, 1666-1675 (2006).

61. M. A. Torres, J. L. Dangl, J. D. G. Jones, Arabidopsis gp91(phox) homologues AtrbohD and AtrbohF are required for accumulation of reactive oxygen intermediates in the plant defense response. *P Natl Acad Sci USA* **99**, 517-522 (2002).
62. S. J. Clough, A. F. Bent, Floral dip: a simplified method for Agrobacterium-mediated transformation of Arabidopsis thaliana. *Plant J* **16**, 735-743 (1998).
63. M. Wenig *et al.*, Systemic acquired resistance networks amplify airborne defense cues. *Nat Commun* **10**, (2019).
64. M. Zhou *et al.*, Redox rhythm reinforces the circadian clock to gate immune response. *Nature* **523**, 472-U221 (2015).
65. A. V. Gendrel, Z. Lippman, R. Martienssen, V. Colot, Profiling histone modification patterns in plants using genomic tiling microarrays. *Nat Methods* **2**, 213-218 (2005).
66. S. R. Jaffrey, S. H. Snyder, The biotin switch method for the detection of S-nitrosylated proteins. *Sci STKE* **2001**, pl1 (2001).
67. S. Akter *et al.*, Chemical proteomics reveals new targets of cysteine sulfinic acid reductase. *Nat Chem Biol* **14**, 995-+ (2018).

Acknowledgments:

We thank Dr. Sheng Yang He for *Pst* DC3000 *hrcC*$^-$ and *Pst* DC3000/avrRpt2 bacteria strains; Dr. Jose Pruneda-Paz for WT (*CCA1$_P$:LUC*), *che-1* (*CCA1$_P$:LUC*), *lhy-20* (*CCA1$_P$:LUC*) and *che-1 lhy-20* (*CCA1$_P$:LUC*) mutant lines. We thank Dr. Pei Zhou, Mingru Li and Dr. Christoph F. Schmidt for help in measuring H_2O_2 levels. We also thank Lucas Li at the Duke Proteomics and Metabolomics Core Facility for measuring SA and Pip.

Funding:

National Institutes of Health grant NIH 1R35GM118036 (XD)

National Science Foundation grant NSF IOS-1645589 and IOS-2041378 (XD)

Howard Hughes Medical Institute (XD)

Hargitt Postdoctoral Fellowship (LC, HY)

Author contributions:

Conceptualization: LC, HY, XD

Methodology: LC, TC, XD

Investigation: LC, HY, TC, MM, XZ

Funding acquisition: LC, HY, XD

Supervision: XD

Writing – original draft: LC, XD

Writing – review & editing: LC, HY, TC, XZ, XD

Competing interests:

XD is a founder of Upstream Biotechnology Inc. and a member of its scientific advisory board, as well as a scientific advisory board member of Inari Agriculture Inc. and Aferna Bio.

Data and materials availability: All generated materials in the manuscript are available upon request. All data are available in the main text or the supplementary materials.

Supplementary Materials

Materials and Methods

Figs. S1 to S8

Tables S1 to S3

Movies S1 to S3

Fig1

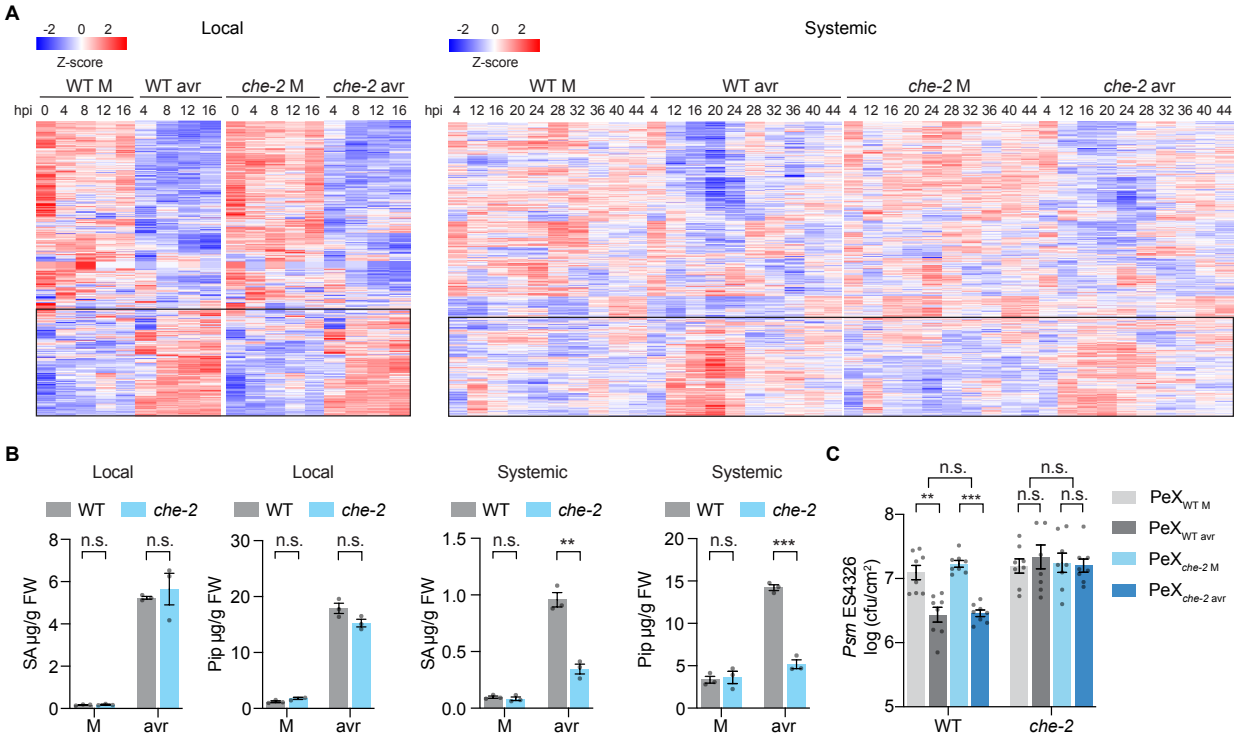

Fig. 1. CHE functions specifically in the systemic tissues during SAR. (**A**) Heatmaps of normalized RASL-seq reads in local and systemic tissues after mock (M; 10 mM $MgCl_2$) or *Psm* ES4326/avrRpt2 (avr; OD_{600nm} = 0.01) treatment. Black rectangles highlight the reads of upregulated genes by the avr treatment. hpi, hours post infiltration. (**B**) Levels of SA and Pip in local (12 hpi) and systemic tissues (24 hpi). Data are means ± SEMs (n = 3). (**C**) Bacterial growth in WT and *che-2* plants pre-treated with petiole exudate (PeX) collected from WT or *che-2* plants after M or avr treatment. Data are means ± SEMs (n = 8). Significant differences were calculated using either two-tailed Student's t-tests or two-way ANOVA. ***P < 0.001; **P < 0.01; *P < 0.05; n.s., not significant.

Fig 2

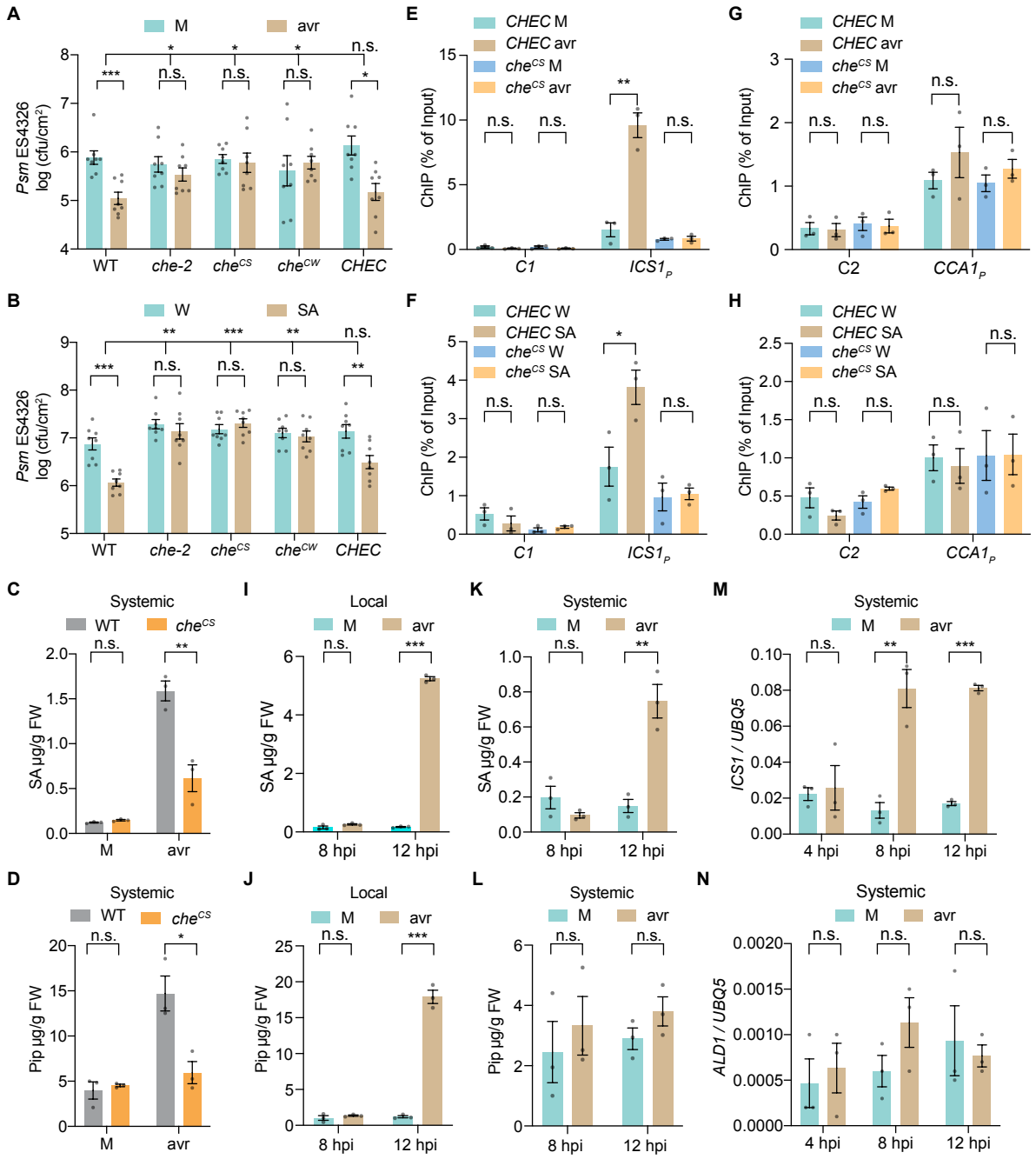

482

483 **Fig. 2. The cysteine residue in CHE is required for systemic SA synthesis, Pip accumulation,**
484 **and SAR.** (**A**) Bacterial growth in systemic tissue after local pathogen induction. Plants were
485 infiltrated with mock (M; 10 mM $MgCl_2$) or *Psm* ES4326/avrRpt2 (avr; OD_{600nm} = 0.01) 2 days
486 before infiltration of the systemic tissues with *Psm* ES4326 (OD_{600nm} = 0.001), and bacterial
487 growth was measured 3 days after the second infiltration. Data are means ± SEMs (n = 8). *CHEC*,
488 *che-2* transformed with the WT *CHE* expressed by its native promoter. che^{CS} and che^{CW},
489 transformants expressing the cysteine-to-serine and cysteine-to-tryptophan mutant *che*,

respectively. (**B**) Bacterial growth after SA treatment. Plants were sprayed with water (W) or 1 mM SA 1 day before infiltration of *Psm* ES4326, and bacterial growth was measured 3 days after the infiltration. Data are means ± SEMs ($n = 8$). (**C** and **D**) Levels of SA (C) and Pip (D) in systemic tissues after local M or avr treatments. Data are means ± SEMs ($n = 3$). (**E** and **F**) ChIP-qPCR analysis of CHE binding to the *ICS1* promoter carrying the TCP-binding site ($ICS1_P$) using systemic tissues after local M or avr treatment (E) and W- or SA-treated tissues (F). *C1*, control for *ICS1p*. Data are means ± SEMs ($n = 3$). (**G** and **H**) ChIP-qPCR analysis of CHE binding to the *CCA1* promoter carrying the TCP-binding site ($CCA1_P$) using systemic tissues after local M or avr treatment (G) and W- or SA-treated tissues (H). *C2*, control for *CCA1p*. Data are means ± SEMs ($n = 3$). (**I** and **J**) Time-course measurement of SA (I) and Pip (J) in the local tissues. Data are means ± SEMs ($n = 3$). hpi, hours post infiltration. (**K** and **L**) Time-course measurement of SA (K) and Pip (L) in the systemic tissues. Data are means ± SEMs ($n = 3$). (**M** and **N**) Time-course transcriptional level of *ICS1* (M) and *ALD1* (N) in the systemic tissues of WT plants. Data are means ± SEMs ($n = 3$). Significant differences were calculated using either two-tailed Student's t-tests or two-way ANOVA. ***$P < 0.001$; **$P < 0.01$; *$P < 0.05$; n.s., not significant.

Fig 3

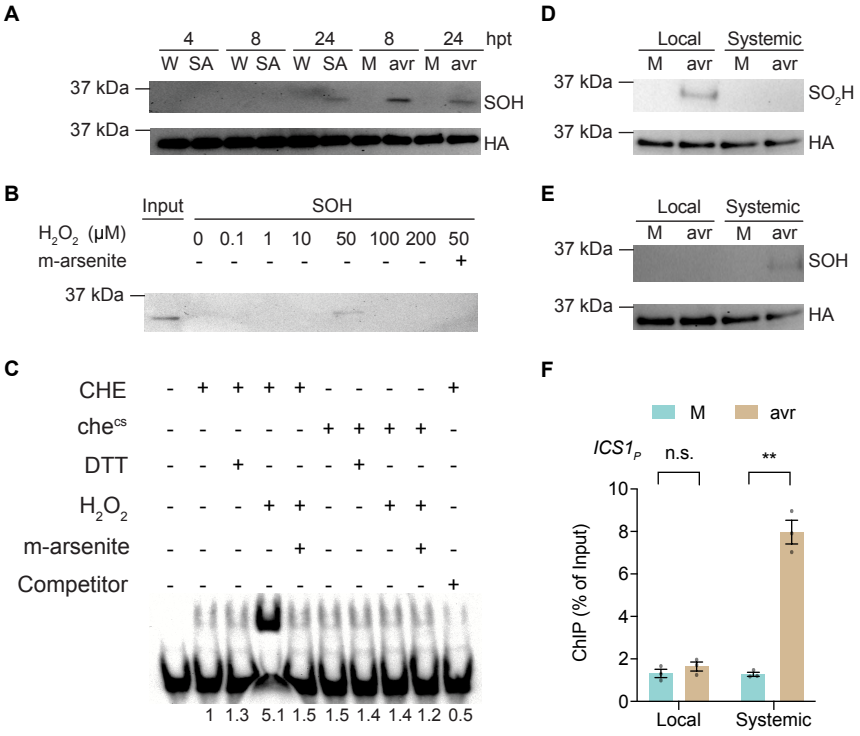

Fig. 3. Sulfenylation of CHE occurs specifically in systemic tissues during SAR. (**A**) Sulfenylation (SOH) of CHE in systemic tissues after local mock (M; 10 mM $MgCl_2$) or *Psm* ES4326/avrRpt2 (avr; OD_{600nm} = 0.01) treatment, or in the tissues after water (W) or 1 mM SA treatment. hpt, hours post treatment. (**B**) *In vitro* sulfenylation of CHE after H_2O_2 treatment and specific removal of sulfenylation by 50 mM sodium arsenite (m-arsenite). (**C**) Electrophoresis mobility shift assay of recombinant CHE protein binding to the DNA probe of TCP-binding site of *ICS1* promoter (*TBSi*). (**D** and **E**) Sulfinylation (SO_2H) (D) and SOH (E) of CHE in local and systemic tissues, respectively, after M or avr treatment. Samples are collected 7 to 8 hours post pathogen treatment. (**F**) ChIP-qPCR analysis of CHE binding to the *ICS1* promoter carrying the TCP-binding site (*ICS1P*) in the local and systemic tissues after M or avr treatments. Data are the means ± SEMs (n = 3). Significant differences were calculated using two-tailed Student's t-tests. $^{**}P < 0.01$; n.s., not significant.

Fig 4

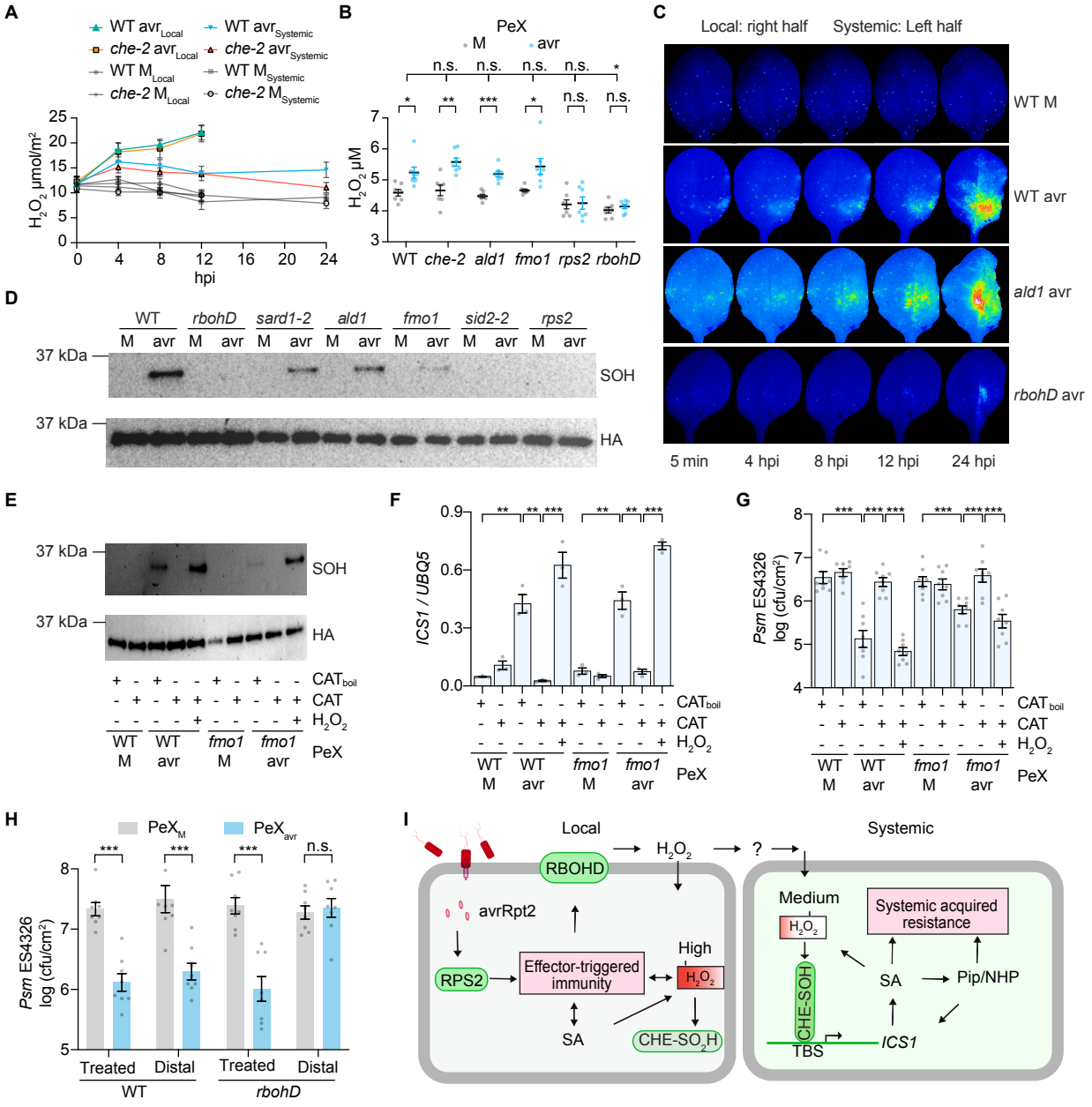

Fig. 4. H_2O_2 produced by RBOHD is the mobile signal that sulfenylates CHE to activate systemic SA synthesis and resistance. (**A**) Time-course measurement of H_2O_2 in local and systemic tissues of plants after mock (M; 10 mM $MgCl_2$) or *Psm* ES4326/avrRpt2 (avr; OD_{600nm} = 0.01) treatment. Data are means ± SEMs (n = 5). hpi, hours post infiltration. (**B**) H_2O_2 levels in petiole exudates (PeX) collected after M or avr treatment. Data are means ± SEMs (n = 7). (**C**) Snap shots from live imaging of ROS production and transportation using 2',7'-dichlorodihydrofluorescein diacetate after treatment with M or avr (also see Movies S1-3). (**D**) Sulfenylation (SOH) of CHE in systemic tissues after local M or avr treatment in different genetic backgrounds. (**E-G**) The effect of catalase treatment of petiole exudates collected after M or avr

530 treatment on CHE sulfenylation (E), *ICS1* expression (F), and bacterial growth (G). Data are means
531 ± SEMs, $n = 3$ for (F), $n = 8$ for (G). (**H**) Bacterial growth in the treated or distal leaves of WT or
532 *rbohD* plants after treatment with PeX collected from WT plants after M or avr treatment. Data
533 are means ± SEMs ($n = 8$). (**I**) The working model of CHE-mediated SAR induction. The
534 perception of bacterial effector avrRpt2 by the immune receptor RPS2 induces ETI and local
535 production of SA, resulting in accumulation of high H_2O_2 concentration and CHE sulfinylation
536 (CHE-SO_2H), which lacks the increased binding activity to the *ICS1* promoter. Local apoplastic
537 H_2O_2 produced and transported/relayed via an unknown mechanism (?) by RBOHD to systemic
538 tissues to sulfenylate CHE (CHE-SOH). CHE-SOH binds to *ICS1* promoter to induce *de novo* SA
539 synthesis and initiate SAR. Full-scale resistance is achieved through an amplification loop
540 involving synergistic activities of SA and Pip/NHP. Significant differences were calculated using
541 either two-tailed Student's t-tests or two-way ANOVA. ***$P < 0.001$; **$P < 0.01$; *$P < 0.05$; n.s.,
542 not significant.

543

544 **Materials and Methods**

545 Plant materials

546 *Arabidopsis thaliana*, including wild type (WT), *che-2* (*21*), *che-1* (*21*), *che-3* (SALK_106694),
547 *lhy-20* (*21*), *ald1 (59)*, *fmo1 (60)*, *rps2* (*43, 44*), *sid2-2 (45)*, *rbohD (61)*, *sard1-2* (*20*), and other
548 transgenic plants used in this study are all in the Columbia-0 ecotype background. Plants were
549 grown in soil at 22 ºC under 12 hours light/12 hours dark with 60% relative humidity.

550 Plasmid construction and plant transformation

551 To generate CHE complementation lines (*CHEC*), the *CHE* native promoter driving the coding
552 sequence was used to transform *che-2*. Fragments were PCR amplified from the genomic DNA
553 and cloned into pDONR207 with Gateway™ BP Clonase™ II Enzyme Mix (ThermoFisher
554 Scientific) and then cloned into pGWB513 with Gateway™ LR Clonase™ II Enzyme Mix
555 (ThermoFisher Scientific) for plant transformation. Vectors of cysteine mutants (cysteine mutated
556 to serine in che^{CS} and cysteine mutated to tryptophan in che^{CW}) were generated through PCR
557 amplification with corresponding primers (Table S1) using pGWB513 carrying *CHEC* as the
558 template, then the *CHEC* template vector were removed by digestion with DpnI (NEB) and the
559 cysteine mutant vectors were recovered by re-transformation in DH5α competent cells. WT or
560 che^{CS} coding sequence was constructed into pGEX6P1-DEST-HA and used for protein expression
561 and purification in *E. coli*. Native promoter-driven the coding sequence of WT or che^{CS} cloned
562 into pGWB513 was used for transformation of *che-1* (*CCA1P:LUC*) and *che-1 lhy-20*
563 (*CCA1P:LUC*) mutants. Native promoter-driven WT CHE coding sequence cloned into pGWB513
564 was used for transformation of *rbohD*, *sard1-2*, *ald1*, *fmo1*, *sid2-2*, and *rps2* mutants. All plasmids
565 constructed were confirmed by Sanger sequencing before use. *Agrobacterium*-mediated
566 transformation was performed as described (*62*).

567 RASL-seq

568 Total RNA extracted using TRIzol (Ambion) was processed as described (*19*). Primers used in
569 RASL-seq are listed in Tables S2 and S3. The raw sequencing data were first aligned to gene-
570 specific primers. The gene counts were subjected to library size normalization and log2
571 transformation. The resulting gene expression matrix is provided in Tables S2 and S3.

572 Quantitative real-time PCR

573 Total RNA was extract from leaf tissues of 3-week-old plants using TRIzol, followed by DNase I
574 (Invitrogen) treatment to remove genomic DNA contamination. The extracted RNA was then used
575 as a template for reverse transcription using SuperScript® III Reverse Transcriptase (Invitrogen)
576 with an oligo (dT) primer. FastStart Universal SYBR Green Master (Roche) was used in real-time
577 PCR with primers listed in Table S1. *Ubiquitin 5* (*UBQ5*) was used as the internal control.

578 SA and Pip quantification

579 SA and Pip were measured as described (*17*) with modifications. 3-6 leaves were collected,
580 weighed, and ground in liquid nitrogen. The samples were then extracted in 1 mL of MeOH/H_2O
581 (80/20, v/v), then vortexed for 1 min and incubated at 4 ºC for 10 min with rotation. The
582 supernatant was collected after centrifugation at 4 ºC (14,000 g for 10 min). The extraction was
583 repeated one more time before combining the two-extracted supernatants into a 2-mL tube, then
584 the supernatant was collected after another centrifugation. 400-800 µL of the extract was
585 evaporated to dryness using an Eppendorf concentrator plus/Vacufuge® plus system. Then, 100
586 µL of a 50 % methanol solution was added into the sample vials and vigorously vortexed. The
587 solution was subjected to centrifugation at 5 °C (15,000 rpm for 5 min) and 40 µL of the resulting
588 supernatant was transferred into the well of a 1 mL 96-well NUNC plate (ThermoFisher Scientific).
589 After adding 10 µL internal mixture (0.5 µg/mL salicylic acid-d_4 and 0.5 µg/mL pipecolic acid-
590 d_9), the plate was mixed on a ThermoMixer at 1,000 rpm for 10 min, then centrifuged at 3,000 rpm
591 for 2 min before injection into the instrument.

592 Samples were analyzed with the Waters TQ-X MS system (Milford, MA) with the Acquity UPLC.
593 Software Masslynx 4.2 was used for data acquisition. The LC separation was performed on a
594 Waters Acquity CSH phenyl-hexyl column (2.1 x 100 mm, 1.7 µm) with mobile phase A (0.1 %
595 formic acid in water) and mobile phase B (0.1 % formic acid in acetonitrile). The flow rate was
596 0.45 mL/min. The linear gradient was as follows: 0-1 min, 100 % A; 3 min, 50 % A; 3.1-4.5 min,
597 0 % A; 4.6-6.1 min, 100 % A. The autosampler was set at 10 °C and the column was kept at 45 °C.
598 The injection volume was 2 µL. Mass spectra were acquired under both positive and negative
599 electrospray ionization (ESI) with MRM as the detection approach. The positive mode was used
600 for pipecolic acid (m/z 130.0 → m/z 67.0) and internal standard pipecolic acid-d_9 (m/z 139.0 →
601 m/z 61.0). The negative mode was used for salicylic acid (m/z 137.0 → m/z 93.0) and internal
602 standard salicylic acid-d_4 (m/z 141.0 → m/z 97.0).

603 <u>Petiole exudate collection and treatment</u>

604 The petiole exudate (PeX) was collected as previously described (*63*) with modifications.
605 Specifically, we first tried two different concentrations of *Psm* ES4326/avrRpt2 (OD_{600nm} = 0.01
606 and OD_{600nm} = 0.0005) to inoculate 3-week-old plant leaves, and excised the leaves at 8 and 24
607 hours, respectively, for PeX collection for 48 hours. We found that after proper dilution, both
608 inoculants produced similar results in H_2O_2 production, CHE sulfenylation and plant defense
609 against *Psm* ES4326. Consequently, we used OD_{600nm} = 0.0005 to simulate a natural infection
610 more closely for the experiments. Another change made in this study was the inclusion of 0.02 %
611 acetanilide in the collection solution to stabilize H_2O_2. The collected PeXs were then used to treat
612 plants, from which leaf samples were collected 4 hours after PeX treatment for protein
613 sulfenylation analysis or 24 hours after PeX treatment for bacterial growth and quantitative real-
614 time PCR analysis. 50 µl of the PeX was used to quantify H_2O_2 concentration. To remove H_2O_2
615 from the PeX, 0.1 mg/mL catalase (Sigma) was used. To denature catalase, the catalase solution
616 was incubated at 95 ºC for 15 min. To rescue the catalase-treated PeX, an Amicon® Ultra-4
617 centrifugal filter (Millipore) was used to remove the enzyme, and 10 µM H_2O_2 was added to the
618 collected PeX.

619 <u>ETI-induction of SAR and measurement of bacterial growth</u>

620 SAR was induced by infiltrating half-leaf with *Psm* ES4326/avrRpt2 (OD_{600nm} = 0.01) as the local
621 tissues and the other un-infiltrated half-leaf was used as the systemic tissues (except specific
622 mentioned) for RASL-seq, SA and Pip production quantifications, quantitative real-time PCR, the
623 sulfenylation and sulfinylation of CHE, chromatin immunoprecipitation, H_2O_2 production assay,
624 and ROS production assays. Plants were also infiltrated with *Pst* DC3000 *hrcC*$^-$ (OD_{600nm} = 0.01)
625 and *Pst* DC3000/avrRpt2 (OD_{600nm} = 0.01) using half-leaf and samples were collected 24 hours
626 after infiltration for the sulfenylation of CHE and quantitative real-time PCR assays.

627 For examining SAR protection against bacterial growth, 3-week-old plants were first infiltrated
628 with 10 mM $MgCl_2$ (M) or *Psm* ES4326/avrRpt2 (OD_{600nm} = 0.01). After 2 days, the systemic
629 leaves were infiltrated with *Psm* ES4326 (OD_{600nm} = 0.001). Bacterial growth was measured 3
630 days after the second pathogen infection. Two leaf-discs (0.6 cm in diameter) were placed in one
631 of the 8-strip tubes containing 1 metal bead and 500 µL sterilized 10 mM $MgCl_2$ and grind with a
632 SPEX™ SamplePrep 2010 Geno/Grinder™ (ThermoFisher Scientific) at 1500 strokes/min for 30
633 sec for twice. Then, the samples were centrifuged at 2000 rpm for 1 min. 10 × dilution (6 gradient
634 dilutions per sample) was used for each sample. 10 µL aliquots from each dilution were spread on
635 King's B Medium. Allow the bacteria to grow for 2 days at 30 ºC and then count individual colony
636 number for each dilution. The bacteria number were calculated based on the dilution and the area
637 of leaf discs.

638 For petiole exudate (PeX)-triggered plant defense, 3-week-old plants were first infiltrated with
639 PeX. One days after, the treated leaves or distal leaves were infiltrated with *Psm* ES4326 (OD_{600nm}
640 = 0.001) and bacterial growth was measured 3 days after pathogen infection.

641 Luciferase imaging and circadian rhythm calculation

642 Independent T1 seedlings were grown on half strength of Murashige-Skoog (MS) media with 25
643 µg/mL hygromycin B (ThermoFisher Scientific) for 10 days at 22 ºC under 12 hours light/12 hours
644 dark condition. Then they were sprayed with 2.5 mM luciferin (Gold Biotechnology) in 0.02%
645 Triton X-100 (Sigma) and transferred to constant light condition one day before imaging. Imagines
646 were taken every 2 hours with exposure time of 20 min using a charge-coupled device camera
647 (PIXIS 2048). The quantifications of bioluminescence intensity were performed using Image J.
648 Periods of circadian rhythm were inferred from a sine wave as previously described (*64*).

649 Chromatin immunoprecipitation (ChIP)

650 ChIP was performed as previously described (*65*) with minor modifications. Pierce™ Anti-HA
651 magnetic beads (ThermoFisher Scientific) were used for immunoprecipitation (IP) as described in
652 the manufacturer's protocol, and primes used are listed in Table S1.

653 Protein S-sulfenylation and S-sulfinylation

654 Protein S-sulfenylation and S-sulfinylation were measured using a biotin-switch method as
655 described previously (*66, 67*) with modifications. Leaf tissues (2 g) were collected from 3-week-
656 old plants, ground in liquid nitrogen, and suspended in 25 mL HEN buffer [250 mM HEPES-
657 NaOH (pH 7.7), 1 mM EDTA, 0.1 mM neocuproine] supplemented with 1 × protease inhibitor

658 cocktail (Roche), 2 % SDS, and 50 mM MMTS. The sample was then incubated at 50 ºC for 1
659 hour with vortex under dark condition and the supernatant was collected after centrifugation (4 ºC,
660 7830 rpm for 1 hour). The sample was then precipitated and washed with acetone.

661 For detecting S-sulfenylation, the pellet was suspended with 2-5 mL HEN buffer with 1 % SDS
662 and supplied with 2 mM biotin-HPDP and 50 mM sodium arsenite and incubated at 25 ºC for 1
663 hour with vortex under dark condition.

664 For detecting S-sulfinylation, the pellet was suspended in 2-5 mL HEN buffer with 0.4 % SDS
665 supplied with 20 mM DiaAlk (AOBIOUS) and incubated at 37 ºC for 2 hours with vortex under
666 dark condition. The solution is precipitated and washed with acetone and resuspended with HEN
667 buffer supplied with 0.2 mM azide-biotin, 0.1 mM TBTA, and 1 mM $CuSO_4$, and incubated at 25
668 ºC for 2 hours with vortex under dark condition.

669 The subsequent steps were used for detecting both S-sulfenylation and S-sulfinylation. After
670 setting aside 5-10 μL solutions as the input for western blot, the rest solution was precipitated and
671 washed with acetone. The modified protein was pulled down with Pierce™ streptavidin-agarose
672 (ThermoFisher Scientific). The protein was dissolved with 50-100 μL 20 mM HEPES-NaOH
673 buffer, supplied with 1 mM EDTA, 10 mM NaCl, and 100 mM 2-mercaptoethanol. The sample is
674 used for western blot analysis after mixing with 2 × SDS-PAGE buffer and 1 mM DTT.

675 Protein purification and electrophoretic mobility shift assay (EMSA)

676 The CHE protein fused with glutathione-S-transferase (GST) was expressed in *E. coli* strain BL21
677 and purified using Pierce™ glutathione magnetic agarose (ThermoFisher Scientific). The purified
678 protein was digested with PreScission Protease (APEXBIO) to remove GST tag and treated with
679 25 mM DTT or 50 μM H_2O_2 at 25 ºC for 30 min, the treated protein was cleaned up using a Micro
680 Bio-Spin™ P-6 Gel Column (BIO-RAD), and then they were further subjected to 5 mM sodium
681 (meta) arsenite (m-arsenite) treatment at 25 ºC for 30 min (Water treatment was used as the control).
682 The treated protein was cleaned up using a Micro Bio-Spin™ P-6 Gel Column and used for EMSA.
683 EMSA was performed using a LightShift™ Chemiluminescent EMSA kit (ThermoFisher
684 Scientific) following the manufacturer's protocol, and DNA probes used were listed in Table S1.

685 Hydrogen peroxide (H_2O_2) quantification

686 Three leaf discs (0.5 cm in diameter) were collected, grounded in liquid nitrogen, and suspended
687 in 600 μl pre-cooled 20 mM phosphate buffer (pH 6.5) containing 0.02 % acetanilide. After
688 centrifugation at 4 ºC (16,200 g for 10 min), the supernatant was transferred to a new pre-cooled
689 tube. To quantify concentration of H_2O_2, 50 μl of the solution was used according to the protocol
690 provided by Amplex™ Red Hydrogen Peroxide Assay kit (Invitrogen). For each measurement, a
691 H_2O_2 standard curve (0 to 100 μM, each in a volume of 50 ul) were generated. Luminescence was
692 captured using the Victor3 plate reader (PerkinElmer) with excitation at 531 nm and emission
693 detection at 595 nm. The H_2O_2 concentration were determined using the standard curve and divided
694 by the area of the leaf disc. For H_2O_2 collected from PeX, the concentration was determined
695 directly according to the standard curve.

696 Live imaging of reactive oxygen species (ROS)

697 Live ROS imaging was recorded as previously described (*51*) with modifications. 3-week-old plant
698 leaves were infiltrated with 50 μM 2',7'-dichlorodihydrofluorescein diacetate (H_2DCFDA)
699 (Millipore-Sigma) in 50 mM phosphate buffer (pH 7.4) and allowed for 6-8 hours to recover. Then
700 the infiltrated plants were treated with pathogen or mock solution, and images were taken every
701 20 min for 2 days using microscope (LEICA M205 FA). Imaging data were analyzed with ImagJ
702 (FIJI).

703 Statistical analysis

704 Two-tailed Student's t-tests and two-way ANOVA were performed using Graphpad prism 8.
705 Sample size is described in the relevant figure legends and experiments have been performed at
706 least twice with similar results. For SA and Pip measurement, CHIP-qPCR and luciferase imaging,
707 at least 3 independent samples were used in the figures.

708

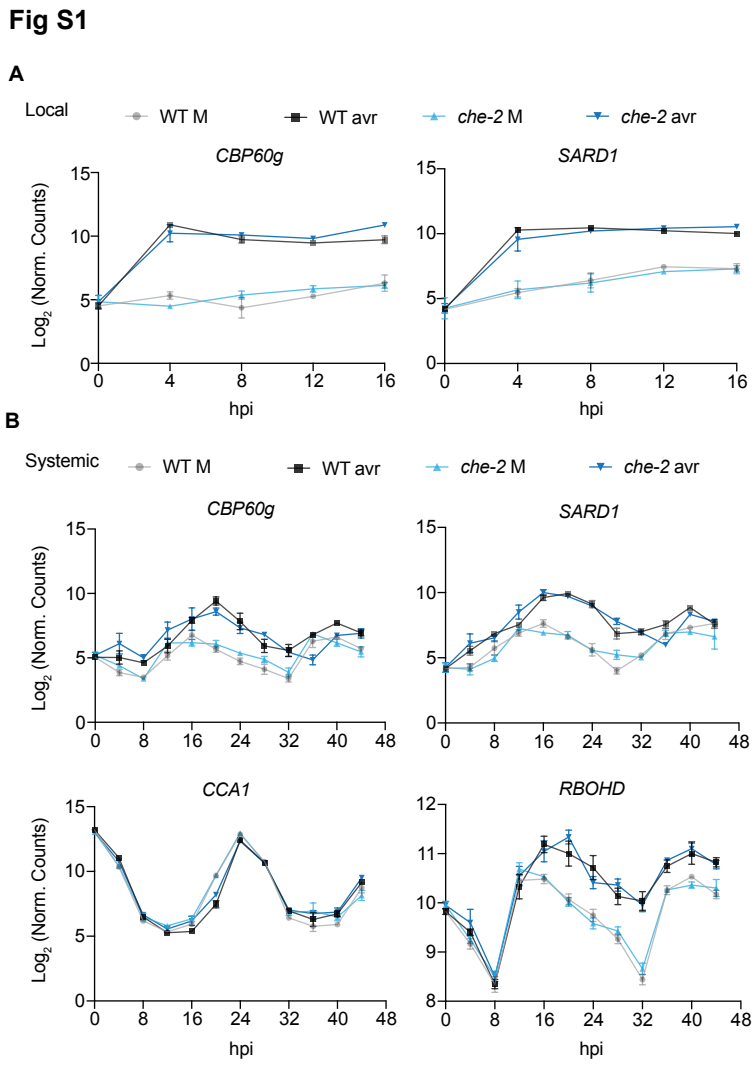

Fig. S1. Normalized read counts from RASL-seq. (**A** and **B**) Normalized transcript read counts in WT and *che-2* plants collected from local (A) and systemic (B) tissues after mock (M; 10 mM $MgCl_2$) or *Psm* ES4326/avrRpt2 (avr; OD_{600nm} = 0.01) treatment. Data are means ± SEMs ($n \geq 3$). hpi, hours post infiltration.

Fig S2

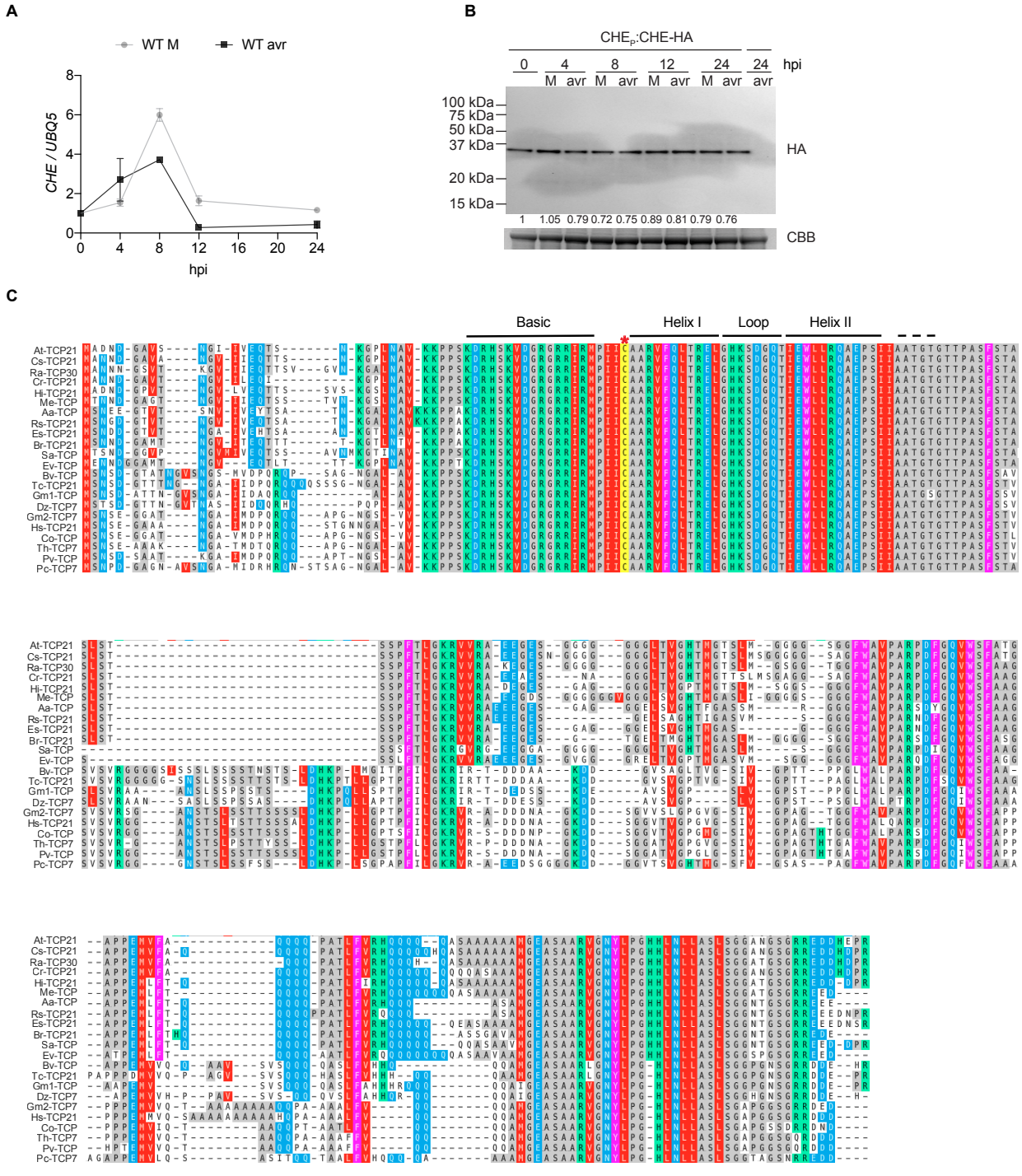

715

716 **Fig. S2. CHE transcript and protein levels and conservation of the cysteine residue in CHE**
717 **among plant species.** (**A** and **B**) CHE transcript (A) and protein level (B) changes in systemic
718 tissues after local mock (M; 10 mM $MgCl_2$) or *Psm* ES4326/avrRpt2 (avr; OD_{600nm} = 0.01)
719 treatment. hpi, hours post infiltration. Data are means ± SEMs. n = 3 for (A). (**C**) Sequence
720 alignment of CHE homologs in plants. The red star indicates the conserved cysteine residue.

721 *Arabidopsis thaliana* (*At*), *Camelina sativa* (*Cs*), *Rorippa aquatica* (*Ra*), *Capsella rubella* (*Cr*),
722 *Hirschfeldia incana* (*Hi*), *Microthlaspi erraticum* (*Me*), *Arabis alpina* (*Aa*), *Raphanus sativus* (*Rs*),
723 *Eutrema salsugineum* (*Es*), *Brassica rapa* (*Br*), *Sinapis alba* (*Sa*), *Eruca vesicaria* (*Ev*), *Bauhinia*
724 *variegate* (*Bv*), *Theobroma cacao* (*Tc*), *Gossypium mustelinum* (*Gm*), *Durio zibethinus* (*Dz*),
725 *Glycine max* (*Gm*), *Hibiscus syriacus* (*Hs*), *Corchorus olitorius* (*Co*), *Tarenaya hassleriana* (*Th*),
726 *Phaseolus vulgaris* (*Pv*), *Prosopis cineraria* (*Pc*).

727

Fig S3

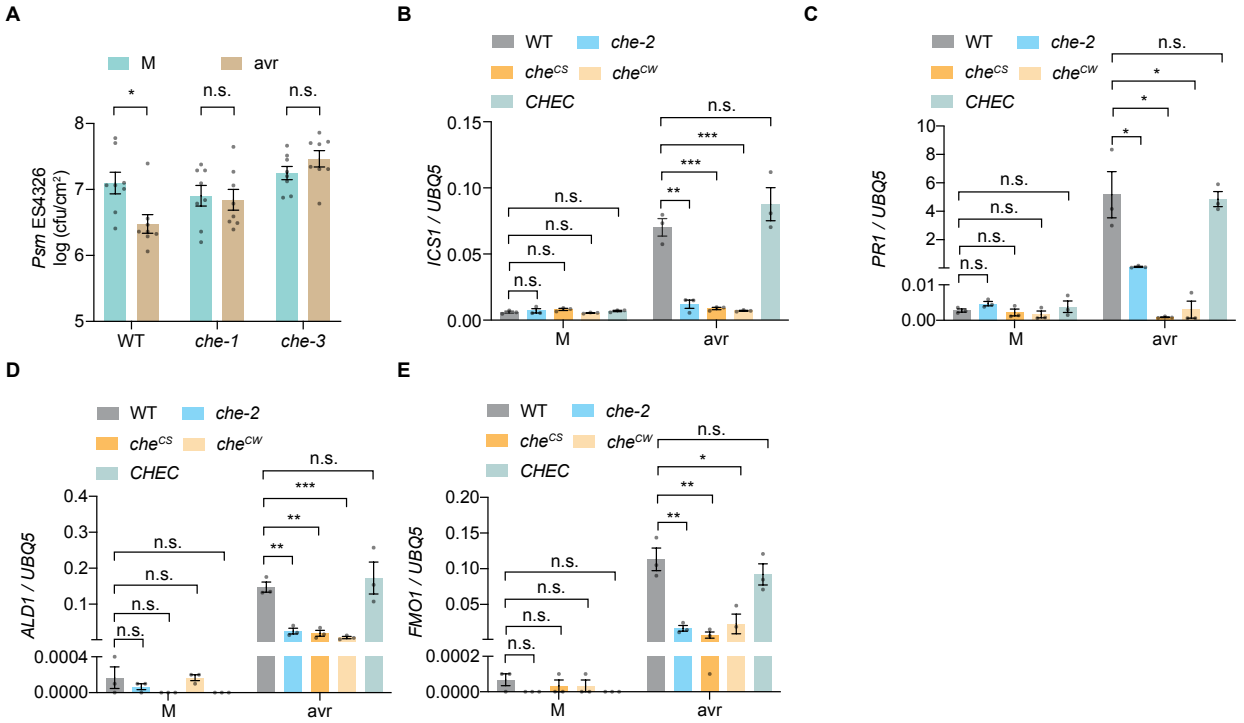

Fig. S3. Bacterial growth and defense-related gene expression in systemic tissues. (**A**) Bacterial growth after pathogen challenge. Plants were infiltrated with mock (M; 10 mM $MgCl_2$) or *Psm* ES4326/avrRpt2 (avr; OD_{600nm} = 0.01) 2 days before infiltration of the systemic tissues with *Psm* ES4326 (OD_{600nm} = 0.001), and bacterial growth was measured 3 days after the second infiltration. Data are means ± SEMs (n = 8). (**B-E**) Transcriptional levels of *ICS1* (B), *ALD1* (C), *FMO1* (D) and *PR1* (E) in systemic tissues after local M or avr treatment. Data are means ± SEMs (n = 3). *CHEC*, *che-2* transformed with the WT *CHE* expressed by its native promoter. che^{CS} and che^{CW}, transformants expressing the cysteine-to-serine and cysteine-to-tryptophan mutant *che*, respectively. Significant differences were calculated using two-tailed Student's t-tests. ***P < 0.001; **P < 0.01; *P < 0.05; n.s., not significant.

Fig S4

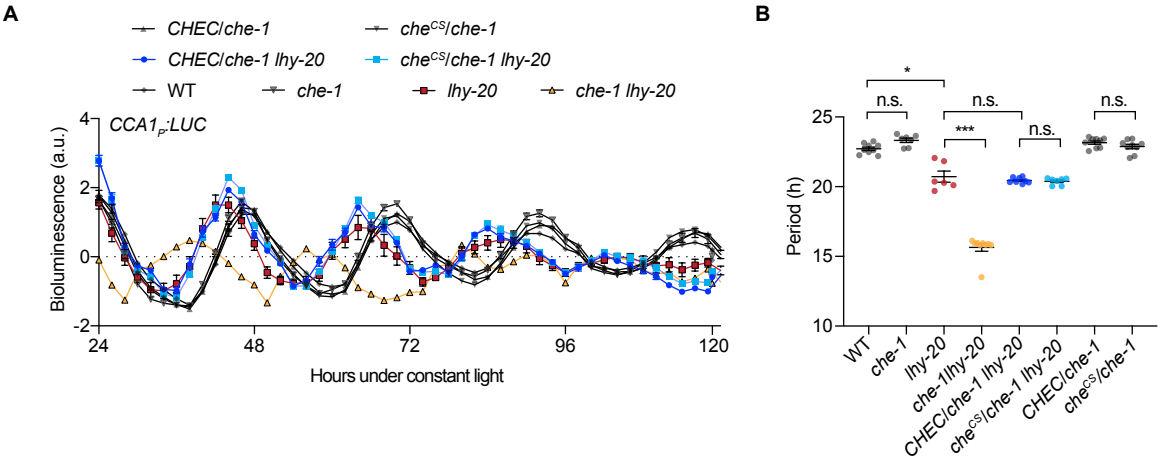

Fig. S4. The cysteine mutant can rescue the phenotype of *che-1* in the regulation of *CCA1*. (**A**) Bioluminescence activity of *CCA1P:LUC* under constant light condition. Data are means ± SEMs ($n \geq 6$). *CHEC/che-1*, *che-1* transformed with the WT *CHE* expressed by its native promoter. *che*^{CS}, transformants expressing the cysteine-to-serine mutant of CHE. (**B**) Period estimates of *CCA1P:LUC* activity. Data are means ± SEMs ($n \geq 6$). Significant differences were calculated using two-tailed Student's t-tests. ***$P < 0.001$; **$P < 0.01$; *$P < 0.05$; n.s., not significant.

Fig S5

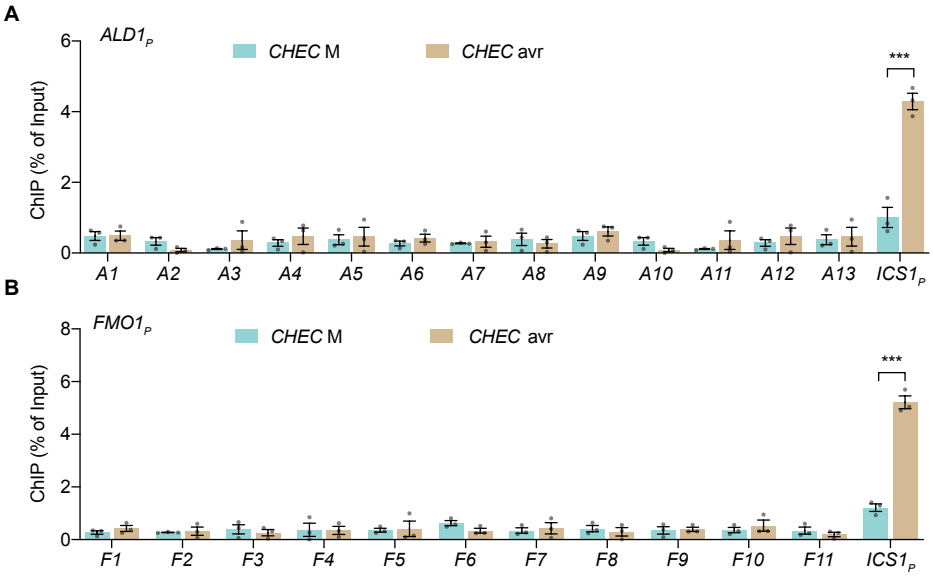

Fig. S5. CHE does not bind to the *ALD1* or *FMO1* promoter. (**A** and **B**) ChIP-qPCR analysis of CHE binding to the *ALD1* promoter (*ALD1P*) (A) and the *FMO1* promoter (*FMO1P*) (B) in systemic tissues 24 hours after local mock (M; 10 mM $MgCl_2$) or *Psm* ES4326/avrRpt2 (avr; OD_{600nm} = 0.01) treatment. *A1* to *A13*, qPCR fragments covering the promoter sequence of *ALD1* (1908 bp upstream ATG to 46 bp downstream ATG); *F1* to *F11*, qPCR fragments covering the promoter sequence of *FMO1* (1583 bp upstream ATG to 53 bp downstream ATG); *ICS1P*, the *ICS1* promoter sequence carrying the TCP-binding site. Data are means ± SEMs (n = 3). Significant differences were calculated using two-tailed Student's t-tests. ***$P < 0.001$.

Fig S6

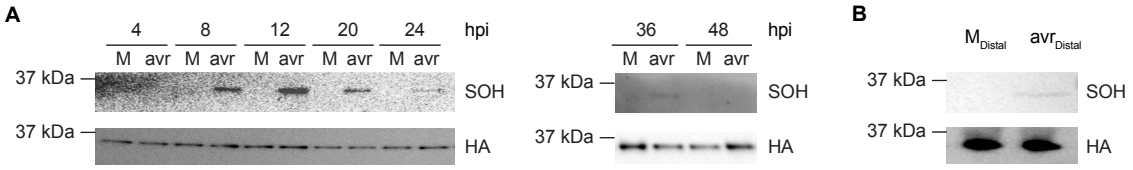

758

759 **Fig. S6. *In vivo* sulfenylation of CHE.** (**A**) Time-course sulfenylation (SOH) of CHE in systemic
760 tissues after local mock (M; 10 mM $MgCl_2$) or *Psm* ES4326/avrRpt2 (avr; OD_{600nm} = 0.01)
761 treatment. hpi, hours post infiltration. (**B**) Sulfenylation of CHE in the distal tissues 24 hours after
762 treatment of the lower leaves with M or avr.

763

Fig S7

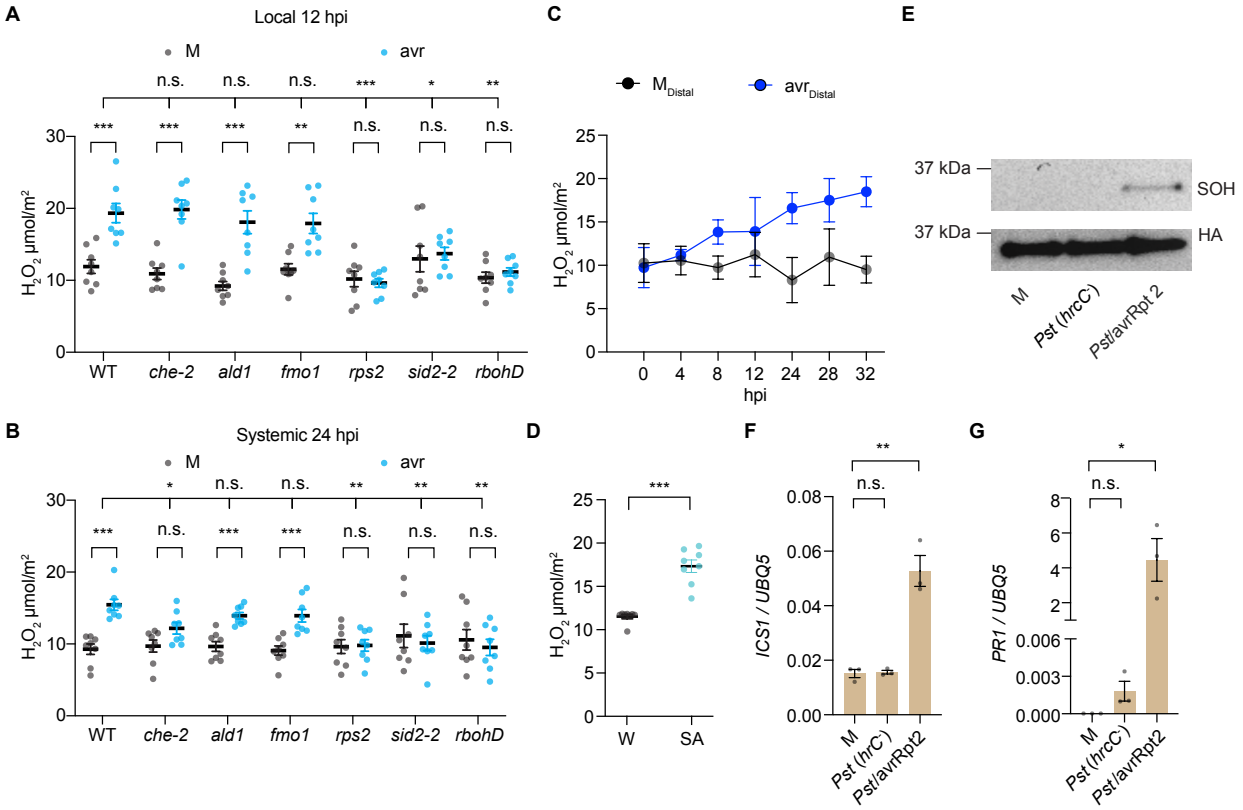

764

765 **Fig. S7. H_2O_2 is the initial mobile signal for ETI-induced SAR.** (**A** and **B**) Levels of H_2O_2
766 produced in the local tissues 12 hours after mock (M; 10 mM $MgCl_2$) or *Psm* ES4326/avrRpt2
767 (avr; OD_{600nm} = 0.01) treatment (A) or in the systemic tissues 24 hours after the local treatment
768 (B). hpi, hours post infiltration. Data are means ± SEMs (n = 8). (**C**) Time-course H_2O_2 production
769 in the distal tissues when lower leaves were treated with M or avr. Data are means ± SEMs (n =
770 5). (**D**) Levels of H_2O_2 produced 24 hours after water (W) or 1 mM SA treatment in WT plants.
771 Data are the means ± SEMs (n = 8). (**E-G**) Sulfenylation of CHE (E) and expressions of *ICS1* (F)
772 and *PR1* (G) in systemic tissues after local treatment with M, *Pst* DC3000 *hrcC*$^-$ [*Pst* (*hrcC*$^-$)] or
773 *Pst* DC3000/avrRpt2 (*Pst*/avrRpt2). Data are means ± SEMs (n = 3). Significant differences were
774 calculated using either two-tailed Student's t-tests or two-way ANOVA. ***$P < 0.001$; **$P < 0.01$;
775 *$P < 0.05$; n.s., not significant.

776

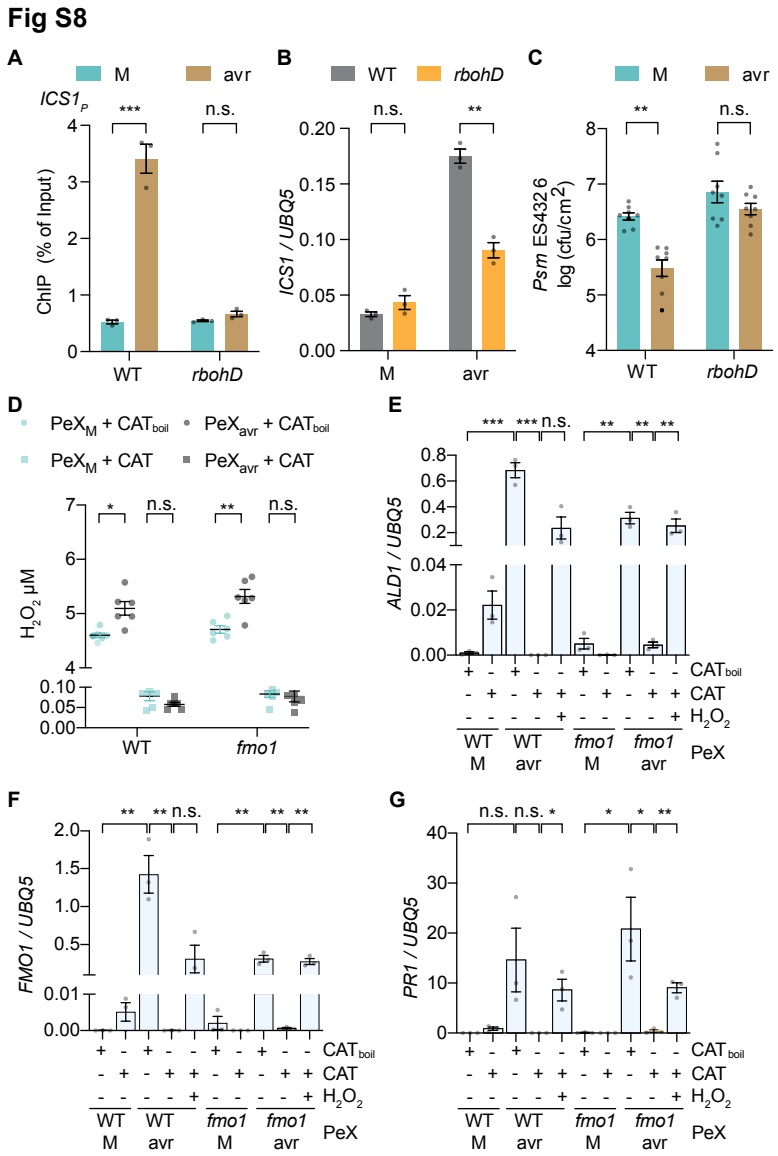

Fig. S8. H_2O_2 produced by RBOHD is the signal that induces systemic SA synthesis and Pip accumulation to confer SAR. (**A-C**) ChIP-qPCR analysis of CHE binding to the *ICS1* promoter carrying the TCP-binding site (*ICS1P*) (A), transcriptional level of *ICS1* (B) and bacterial growth (C) in systemic tissues of WT or *rbohD* plants after local mock (M; 10 mM $MgCl_2$) or *Psm* ES4326/avrRpt2 (avr; OD_{600nm} = 0.01) treatment. Data are means ± SEMs. n = 3 for (A and B), n = 8 for (C). *ICS1P*, the *ICS1* promoter sequence carrying the TCP-binding site. (**D**) Levels of H_2O_2 in petiole exudates (PeX) collected from WT and *fmo1* plants after treatment with catalase (CAT) or heat-denatured catalase (CAT_{boil}). Data are means ± SEMs (n = 6). (**E-G**) The expression of *ALD1* (E), *FMO1* (F) and *PR1* (G) after infiltration with PeX collected from WT or *fmo1* treated with M or avr. Data are means ± SEMs (n = 3). Significant differences were calculated using two-tailed Student's t-tests. ***P < 0.001; **P < 0.01; *P < 0.05; n.s., not significant.